Journal of Marine Science and Technology

Volume 24 | Issue 6 Article 11

CLASSIFICATION OF INTERTIDAL SEDIMENT USING A TWO-STEP PRINCIPAL COMPONENT ANALYSIS (PCA) OF OPTICAL REFLECTANCE: A CASE STUDY IN GANGHWA TIDAL FLATS

Dong-Jae Kwon
Department of Earth system Sciences, Yonsei University, Shinchon-dong, Seodaemun-gu, Seoul, Korea.

Wook Park
Department of Earth system Sciences, Yonsei University, Shinchon-dong, Seodaemun-gu, Seoul, Korea.

Joong-Sun Won
Department of Earth system Sciences, Yonsei University, Shinchon-dong, Seodaemun-gu, Seoul, Korea., jswon@yonsei.ac.kr

CLASSIFICATION OF INTERTIDAL SEDIMENT USING A TWO-STEP PRINCIPAL COMPONENT ANALYSIS (PCA) OF OPTICAL REFLECTANCE: A CASE STUDY IN GANGHWA TIDAL FLATS

Acknowledgements

This research was part of the project titled “Development of Geostationary Ocean Color Imager (GOCI) Land Products for Long-term Monitoring of Tidal Flats and Arid Lands” funded by the Korea Institute of Ocean Science and Technology (KIOST).

Journal of Marine Science and Technology, Vol. 24, No. 6, pp. 1136-1145 (2016)
DOI: 10.6119/JMST-016-1026-2

CLASSIFICATION OF INTERTIDAL SEDIMENT USING A TWO-STEP PRINCIPAL COMPONENT ANALYSIS (PCA) OF OPTICAL REFLECTANCE: A CASE STUDY IN GANGHWA TIDAL FLATS

Dong-Jae Kwon, Wook Park, and Joong-Sun Won

Key words: intertidal flats, grain size, two-step PCA, optical reflectance, LANDSAT OLI.

ABSTRACT

Sediment distribution within intertidal flats varies widely, ranging from mud-dominant to sand-dominant, with extensive seasonal changes. However, retrieving grain size information from remotely sensed data is difficult because the optical reflectance of intertidal sediment is not a function of a single parameter but varies according to water content, grain size, topography, surface water, benthic algae, and halophytes. Among these, grain size and water content are two important parameters. The fact that intertidal sediments are always affected by tide necessitates the development of a water-independent grain size retrieval model. Mud and sand sediment are known to be well distinguished under dry conditions in principal component analysis (PCA) space but hardly distinguished under saturated conditions. Here, we introduce a new grain size retrieval model by removing the water-content dependency from optical reflectance via a two-step PCA transform. To define the relationship between grain size, water content, and optical reflectance, we prepared two different standard samples with different grain sizes by wet sieving. By exploiting simplified reflectance features of the standard samples, we established a two-step PCA transform model. This grain-size retrieval model was applied to LANDSAT-8 images for sediment classification within the Ganghwa tidal flats, South Korea. The results demonstrate that discriminating between sand-dominant and mud-dominant areas on the basis of the model is feasible. Seasonal changes of sediment distribution within the tidal flats are well observed from the results.

Paper submitted 05/27/16; revised 10/06/16; accepted 10/26/16 Author for correspondence: Joong-Sun Won (e-mail: jswon@yonsei.ac.kr).
Department of Earth system Sciences, Yonsei University, Shinchon-dong, Seodaemun-gu, Seoul, Korea.

I. INTRODUCTION

Grain size distributions of intertidal sediment are important to ecological and organic matter and affect pollutant processes (Cracknell, 1999; Rainey et al., 2000). Sedimentary facies of intertidal sediment are affected by tidal energy, river flows, topography, shoreline gradient, etc. Seasonal variations, climate change, bioturbation, and human activities also influence surface sediment distributions. Because a change of intertidal area could substantially affect society, continuous monitoring of such areas is necessary. However, intertidal regions are difficult to access, and conventional mapping by pointwise field samples is spatially unrepresentative because of errors introduced through sediment sampling and subsequent interpolations (Tyler et al., 1996). Instead, remote sensing with appropriate tactics is suitable for mapping intertidal flats. Satellite imagery provides large ground coverage with frequent revisiting capabilities.

The optical reflectance of intertidal sediment can possibly be utilized to classify intertidal grain size. However, measuring grain size directly from optical reflectance is difficult because the reflectance of intertidal sediments is a multi-parameter function that includes grain size, interstitial moisture content, surface water, benthic algae, topography, etc. Examining these parameters requires knowledge of the relationship between each factor and spectral reflectance (Ryu et al., 2004). Thus, establishing a simple classification model or tactics for retrieving grain size of intertidal sediment solely from satellite data is difficult. Among the aforementioned parameters, grain size and water content (interstitial and surface water) play a key role in determining the reflectance of a vegetation-free bare intertidal bottom surface where the sediment grain size is diverse, such as the west coast of Korea (Doerffer and Murphy, 1989; Ryu et al., 2004). However, the intertidal sediment is always affected by tide; therefore, a water-independent grain size retrieval model is needed. Mud and sand sediment reflectance data can be distinguished by principal component analysis (PCA) under dry conditions (Rainey et al., 2000). However, distinguishing such data by simple PCA becomes difficult as the moisture content approaches

saturation (Rainey et al., 2000), and very high moisture content or saturation is particularly prevalent within intertidal flats.

Here, we introduce a new grain size retrieval model by removing the water content dependency from optical reflectance via a two-step PCA (or modified PCA) transform model. The core idea is an axis rotation of the three-dimensional normal PCA space (PC1, PC2, and PC3) until the water-content-dependent axis becomes horizontal. After the contribution of water content to the PCA components has been separated from the other contributions, a model for grain size can be constructed. The developed model is practically useful for space-borne remote sensing because polar orbit satellites are usually operated not by tide series (Moon-synchronous) but by Sun-synchronous orbit. The model was established on the basis of reflectance measured in a laboratory. We collected intertidal sediment samples from the Ganghwa tidal flats, South Korea, and measured their water content, grain size, and optical reflectance. A simplified model of the relationship between grain size, water content, and optical reflectance was obtained from laboratory measurements. Two-step PCA transform coefficients were then calculated from the simplified model via axis rotation of the PCA. The proposed method was applied to LANDSAT-8 images for intertidal sediment classification of the Ganghwa tidal flats. The application results demonstrate a potential use of the two-step PCA method (or modified PCA) for classification of intertidal sediment and for the study of seasonal changes of sediment distribution. This paper is organized as follows. Section II describes the study area and the proposed method. The core idea of the new method and details of processing are addressed. Section III provides the results obtained when the proposed two-step PCA approach was applied to LANDSAT-8 images to demonstrate its effectiveness. Conclusions and discussion follow in Section IV.

II. STUDY AREA AND METHODOLOGY

1. Study Area

The tidal flats in the west coast of Korea are open-coast tidal flats and have a macro-tidal environment with high tide energy. The tidal current speed and wave influence vary seasonally. Gyeonggi Bay is located on the central western coast of the Korean Peninsula. It receives substantial sediment input from the Han River (Choi and Dalrymple, 2004). The Ganghwa tidal flats, our study area, also receive a large amount of sediment input from the Han River through the Seokmo and Yeomha channels (Fig. 1). Tides are semidiurnal with a mean tidal range of 6.5 m (spring tide approximately of 8 m, neap tide approximately of 4 m) with 25 instances of higher high water and lower high water annually (Woo and Je, 2002). The southern part of the tidal flats, approximately 86% of the Ganghwa tidal flats, between the Yeomha and Seokmo channels is shown in Fig. 1. The surface sedimentary facies are primarily mud flats in the eastern part of the tidal flat, sand flats in the western part, and mixed flats in between (Woo and Je, 2002). The tidal flat in Yeocha-ri (see Fig. 1) consists of very fine sand to coarse silt

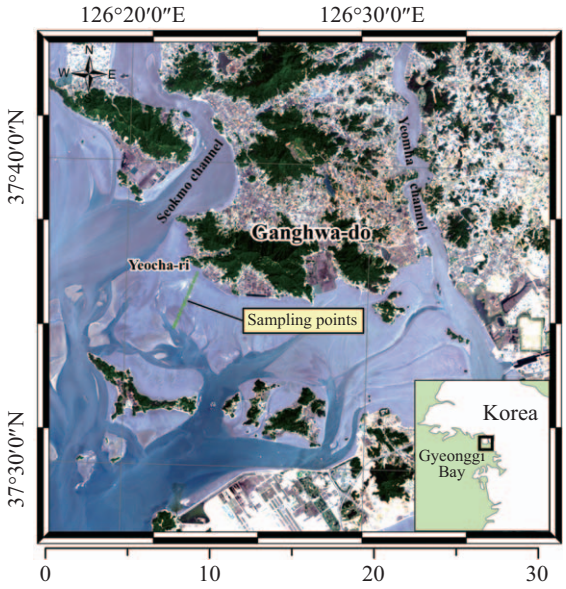

Fig. 1. Location map and the LANDSAT-8 image of the study area; the field survey and sampling line are denoted by green dots.

(3-4 φ), and the fraction of sand increases in the offshore direction. The sediment distribution of this area changes seasonally. A general trend of seasonal variation is that the fraction of mud is the largest in July and gradually becomes coarser until the following spring (Baek, 2010).

2. Field Survey

Field surveys were conducted in the Yeocha-ri tidal flat on 19 November 2013, 30 May 2014, and 22 November 2014. The field survey was chosen as close to the LANDSAT-8 image acquisition date and time on the ebb tide. We collected intertidal sediment samples from the study area and measured their water content, grain size, and optical reflectance. Sampling for laboratory measurement of reflectance as well as in situ reflectance measurement at each sampling site was performed on 30 May 2014. The sampling line (Fig. 1) passes through both mud- and sand-dominant areas, and the total length of the line is approximately 3.6 km.

A total of 60 sediment samples were collected, and their water content, grain size, and optical reflectance were measured for validation. From the sediment samples of the Yeocha-ri intertidal flat, two different standard samples were prepared as per grain size (mud and sand) by wet sieving to obtain a simplified model of the relationship between grain size, water content, and optical reflectance. The water content and optical reflectance of each sample were measured using an Ohaus MB45 and an ASD FieldSpec 3, respectively. To remove organic matter and carbonate, samples were treated with hydrogen peroxide and hydrochloric acid. Their grain size was then measured using a Malvern Mastersizer 2000. The measured grain sizes of the samples used in this study are listed in Table 1. Note that the site numbers in Table 1 correspond to those in Figs. 8-11.

Table 1. Grain sizes at each sampling site.

	Nov. 2013		May 2014		Nov. 2014	
Site no.	Mud (vol %)	Sand (vol %)	Mud (vol %)	Sand (vol %)	Mud (vol %)	Sand (vol %)
A02	60.69	39.29	53.24	46.76	57.03	42.95
A03	44.82	55.18	56.75	43.26	45.19	54.81
A04	40.04	59.95	45.21	54.79	36.42	63.59
A05	25.17	74.83	45.10	54.89	27.09	72.90
A06	18.87	81.13	33.55	66.45	15.41	84.59
A07	14.72	85.27	33.24	66.76	21.71	78.29
A08	20.57	79.43	37.96	62.04	23.65	76.36
A09	19.36	80.64	38.00	62.00	27.36	72.63
A10	45.56	54.43	36.75	63.25	30.86	69.14
A11	24.79	75.21	22.71	77.29	14.77	85.23
A12	19.04	80.95	31.99	68.01	15.28	84.72
A13	9.77	90.23	-	-	-	-
A14	12.02	87.99	38.81	61.19	24.48	75.51
A15	2.63	97.37	3.90	96.10	5.65	94.34
A16	8.33	91.68	6.10	93.91	8.93	91.07
A17	13.59	86.40	19.81	80.18	3.72	96.27
A18	11.26	88.74	3.42	96.57	10.33	89.66
A19	6.33	93.67	8.23	91.77	12.53	87.47
A20	29.79	70.22	8.84	91.16	24.88	75.13
A21	-	-	0.00	100.00	2.53	97.47
A22	-	-	-	-	8.46	91.54
A23	-	-	-	-	12.40	87.60
A24	-	-	-	-	11.65	88.36

Although we attempted to collect surface sediment samples with thicknesses of a few centimeters, some differences are observed between in situ measured reflectance (30 May 2014) and laboratory-measured reflectance of sediment samples taken from the same site. The reflectance values measured in the laboratory are generally lower than those measured in situ. We assume that this difference resulted from disturbance upon sampling. Mixing and compaction of the sampled sediment might slightly distort the natural water content.

3. Core Idea of Two-Step PCA

A lower water content results in a higher spectral contrast between sand and mud in the PCA plane (Rainey et al., 2000). Soil reflectance is well known to initially decrease with increasing water content up to a certain amount and then increase with a further increase in water content (Neema et al., 1987; Liu et al., 2001) However, the positive relationship appears only when soil moisture is oversaturated, which is realized under surface water cover condition in intertidal flats. Thus, the sediment reflectance within intertidal flats can be reasonably assumed to decrease with an increase in water content up to the saturated condition. In this case, the spectral effect in relation to grain size becomes clear at lower water contents when PCA is applied to spectral reflectance. If an optical reflectance model is independent of water content, then the model can be applied to sediment classification. Normal PCA of sediment reflectance does not usually provide water-independent components. However, a new principal component pair, of which one is highly correlated with water content and the other is correlated with grain size, can be derived. The core idea of the proposed method is to apply three-dimensional axis rotation of the principal component space until the water-content-independent axis is found. We refer to this method as "two-step PCA" (or modified PCA) because it consists of two processing steps—a normal PCA transform and a subsequent axis rotation—to achieve modified PCA components.

4. Laboratory Reflectance Measurements

Constructing a water-content-independent model requires measurement of sediment reflectance under water-content-controlled conditions in a laboratory. We conducted laboratory reflectance measurements using the following procedure.

We first prepared two standard sediment samples (mud < 63 μm in grain size; sand > 63 μm in grain size) to define the relationship between water content and spectral reflectance with respect to grain size (Folk, 1966). The grain size class in this study follows the Wentworth grain size classification, which is the most commonly used classification for sediments. The canonical definition of sediment grain sizes generally follows the grain size classification defined by Wentworth (1922). On

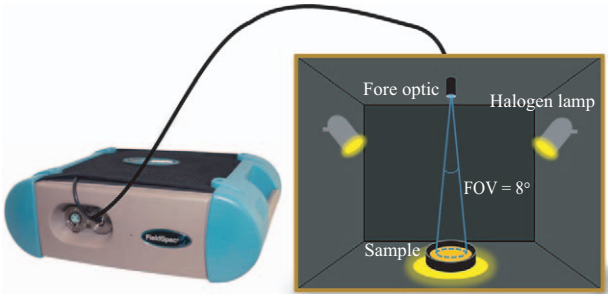

Fig. 2. Illustration of the laboratory measurement setup.

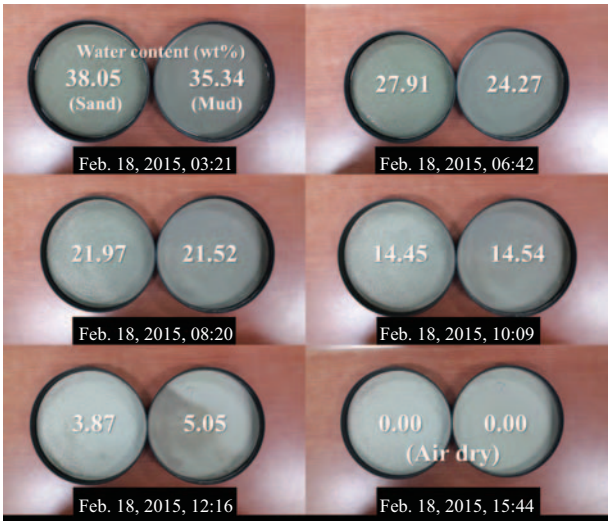

Fig. 3. Standard mud and sand samples at different water content conditions.

the basis of the Wentworth grain size classification, the grain size of sand ranges from 63 μm to 2 mm, whereas that of silt ranges from 3.9 μm to 63 μm. Thus, we chose 63 μm as the threshold of discrimination between mud and sand surface types.

Second, each standard sample was placed in an 18 cm wide and 0.8 cm thick round stainless steel tray. The tray was weighed and painted with Krylon camouflage black paint to minimize reflectance contamination. Distilled water was added until both standard samples were oversaturated.

Third, spectral reflectance measurements of each sample were conducted in the laboratory using an ASD FieldSpec 3 with a dark box (Fig. 2). To simulate natural tidal flat surface conditions, the standard samples were dried at room temperature. The spectral reflectance of a standard sample was measured every 20-30 min until it reached the air-dry condition (Fig. 3). The effects of solid aggregation of small particles were not considered (Cooper and Mustard, 1999).

The laboratory-measured spectral reflectance of the standard samples are shown in Figs. 4(a) and (b). The data were convolved using the LANDSAT-8 Operational Land Imager (OLI) spectral response function; the results are presented in Figs. 4(c) and (d).

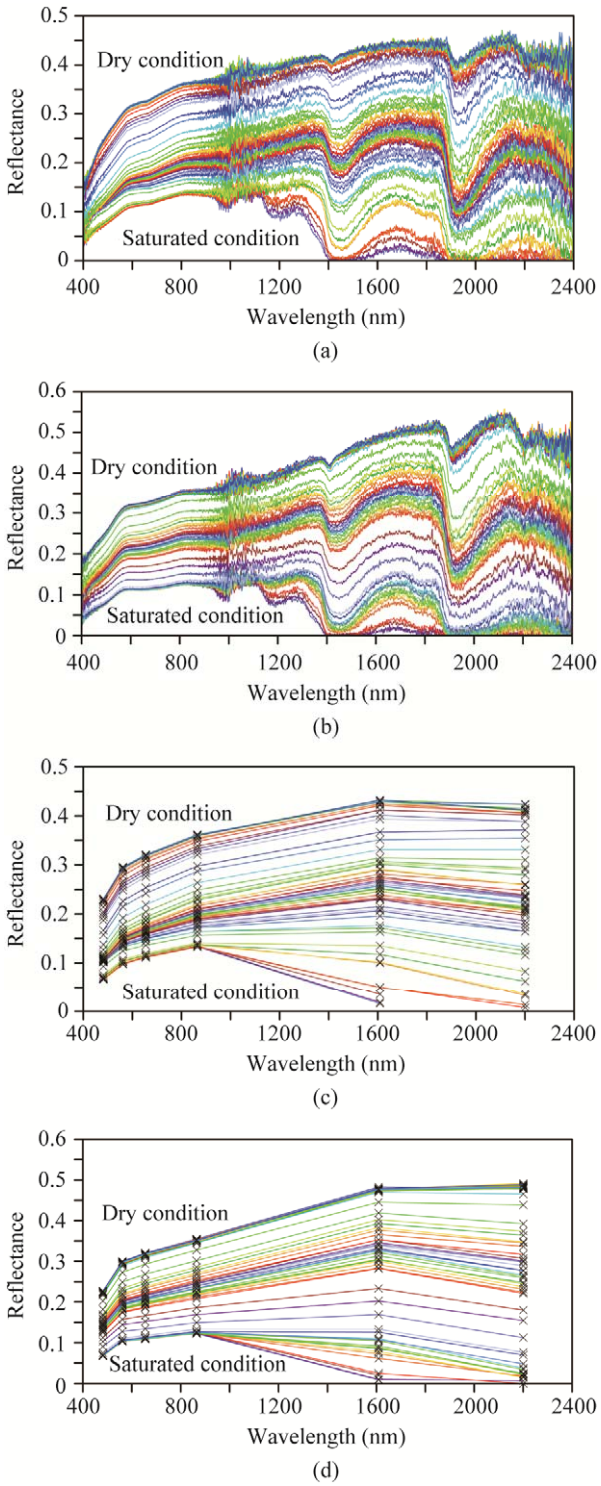

Fig. 4. Laboratory-measured spectral reflectance of the standard samples of mud (a) and sand (b). Simulated spectral reflectance of mud (c) and sand (d) through convolution of the laboratory measured spectral reflectance (a) and (b) using LANDSAT-8 OLI spectral response functions.

LANDSAT-8 OLI bands 2-7 (Table 2) were used in the PCA. To establish a reflectance model of grain size and water content,

Table 2. Specification of LANDSAT-8 OLI spectral bands.

Band no.	Band width (μm)	Ground resolution (m)	Remarks
1	0.435-0.451	30	Coastal/Aerosol
2	0.452-0.512	30	Blue
3	0.533-0.590	30	Green
4	0.636-0.673	30	Red
5	0.851-0.879	30	NIR
6	1.566-1.651	30	SWIR-1
7	2.107-2.294	30	SWIR-2
8	0.503-0.676	15	Pan
9	1.363-1.384	30	Cirrus

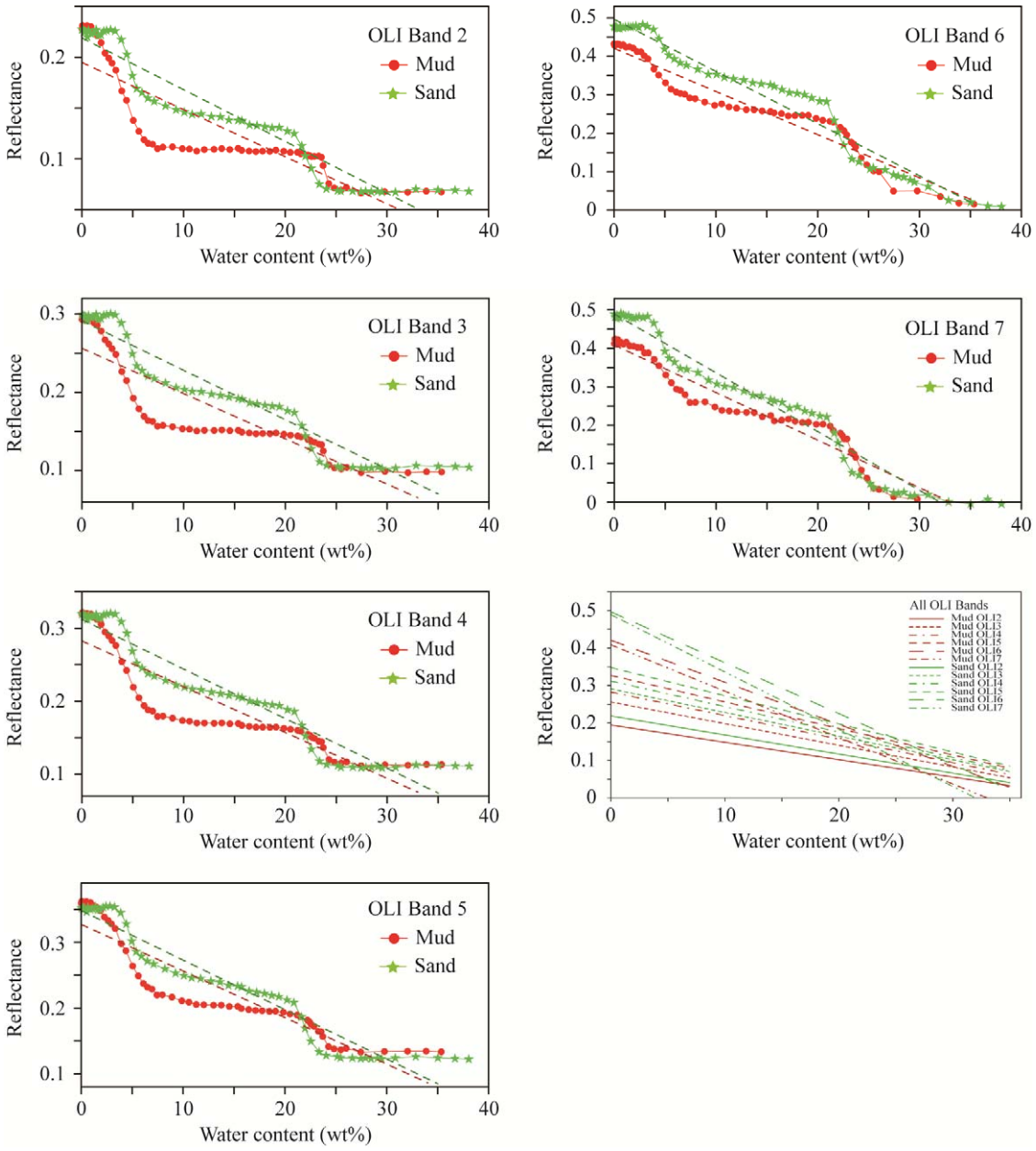

Fig. 5. (Upper six plots) Reflectance of each LANDSAT-8 OLI band versus water content. (Lower) A linear reflectance model for LANDSAT-8 OLI modelled by linear regression with respect to water content.

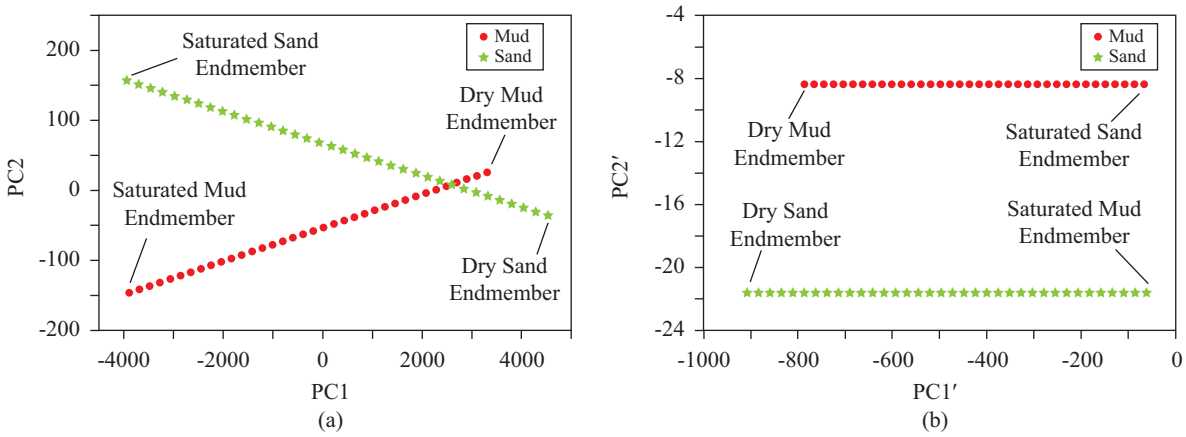

Fig. 6. (a) Projection of PCA of the linear reflectance model in Fig. 5 onto the PC1–PC2 plane. Note that the PC3 axis is normal to the paper. (b) Expression of mud and sand in the modified PC1–PC2 plane that is made by a series of rotations of the original PCA axes. Note that the modified PC2 component is now independent of water content.

Table 3. Two-step PCA coefficients for LANDSAT-8 OLI.

	Modified PC1	Modified PC2
Band 2	-0.21679	-0.16975
Band 3	-0.26963	-0.62576
Band 4	-0.29142	-0.09064
Band 5	-0.32547	0.645932
Band 6	-0.55408	-0.27434
Band 7	-0.61842	0.280902

we fit these datasets using a linear regression for each band (Fig. 5). We then applied this model for the range of water content between 0 and 35% (weight %) because a water content greater than 35% represents the fully saturated condition with surface water cover. The results in Fig. 5 demonstrate that a simple linear model between optical reflectance and water content can be applied.

5. Two-Step PCA Model

A normal PCA transform was first applied to the linearized data (Fig. 5 lower) of the six simulated LANDSAT-8 OLI bands (OLI bands 2-7) to obtain the coefficients of the two-step PCA model. Fig. 6(a) presents a projection of PCA-transformed data onto the PC1-PC2 plane. Note that the PC3 axis is normal to the paper. In Fig. 6(a), the reflectance patterns and end-members of mud and sand are well understood. The negative end-members (left ends) of mud and sand represent the saturated conditions, whereas the positive end-members (right ends) represent the dry conditions. As evident in Fig. 6(a), the reflectance of mud and sand is a function of the water content (or interstitial moisture content) as well as the grain size. Thus, using normal PCA to classify surface sediment into mud and sand is difficult; the two lines should be made independent of water content. For reduction of the water-content dependency of the PCA, the three axes (PC1, PC2, and PC3) are rotated until the mud and sand lines become horizontal as in Fig. 6(b), which presents the projection of PCA onto a new PC1′-PC2′ plane after a series of axis rotations. The new PCA components PC1′ and PC2′ are referred to as the modified PC1 and modified PC2, respectively. As evident in Fig. 6(b), the mud and sand lines in the modified PCA plane are independent of water content and they are well separated from each other by the modified PC2 values. Thus, classifying surface sediment into mud and sand according to the modified PC2 component is now possible. The rotation angles for LANDSAT-8 OLI band 2 to band 7 were 307.5° and 179.8°. Finally, the coefficients corresponding to the two-step PCA, including the normal PCA and subsequent axis rotations, are listed in Table 3. Although we provide only the two-step PCA coefficients for LANDSAT-8 OLI data, the same approach could be extended to any remote sensing sensor similar to the OLI.

III. APPLICATION RESULTS

For performance evaluation and validation, we applied the established model to LANDSAT-8 OLI images band 2 (blue) to band 7 (SWIR) acquired over the study area. Three LANDAT-8 OLI images used in this study were acquired on 3 November 2013, 14 May 2014, and 6 November 2014, as close as possible to the field survey dates and on the ebb-tide condition. These images were corrected for atmosphere using ENVI FLAASH with a U.S. standard model. The intertidal sediment is usually oversaturated if the water content exceeds 35%. In this case, the surface water layer is formed. The water-covered areas were excluded as much possible by utilizing LANDSAT-8 OLI band 7 because the SWIR band is highly sensitive to water cover (Figs. 4(a) and (b)). However, because of the limited ground resolution (30 m), small-scaled features such as remnant surface water or very small intertidal creeks were not fully excluded.

Figs. 7(a)-(c) display the sediment distribution maps of the Ganghwa tidal flats retrieved by the proposed method. The red, blue, and green areas indicate sand-dominated, mud-dominated, and intermediate intertidal flats, respectively. The sedimentary

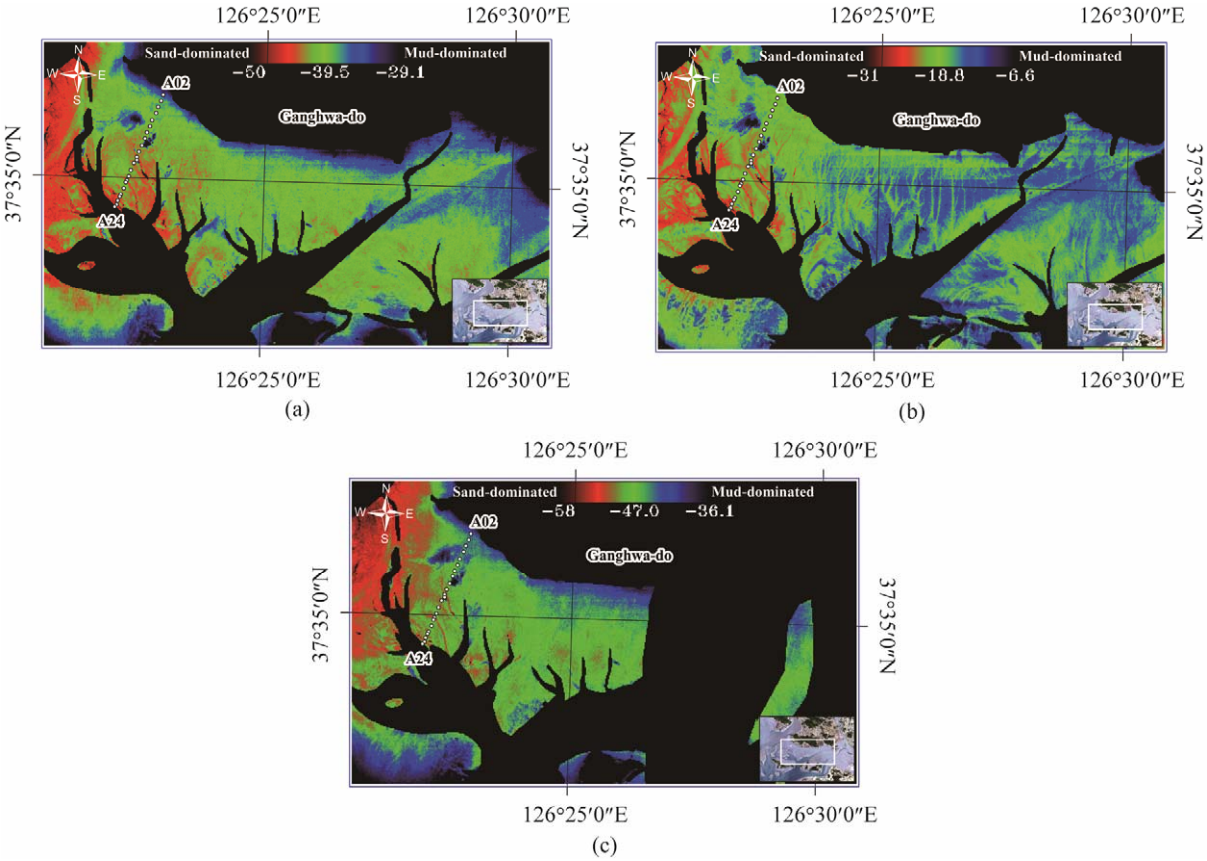

Fig. 7. Grain size distribution map constructed by applying the modified PCA to LANDSAT-8 OLI data acquired on (a) 03 November 2013, (b) 14 May 2014, and (c) 06 November 2014. Seasonal variation pattern, which is sand dominant in winter and mud dominant in summer, is also well observed as well as grain size distribution within the intertidal flat at each period.

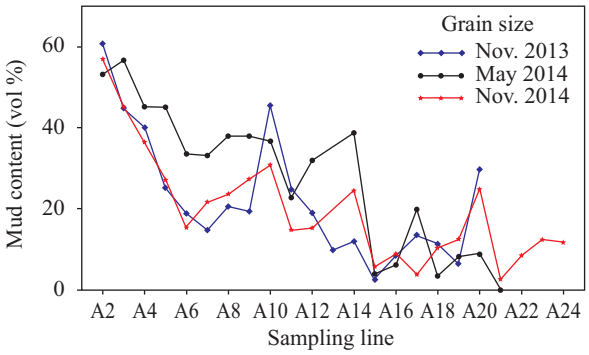

Fig. 8. Variation of mud fraction at each sampling site according to season. The grain size at each sampling site refers to Table 1.

facies within the Ganghwa tidal flat are very well characterized and generally well matched with field surveys. First, the pattern of sediment distribution is well correlated with field observations. Around the Yeocha-ri tidal flat in which field surveys were conducted, all results commonly show increasing sand toward the offshore. As Woo and Je (2002) reported, the surface sedimentary facies are primarily mud in the eastern part of the tidal flat, sand-dominated in the western part, and mixed flats in the area between them. Second, the seasonal variation is also very well observed in the results. The general pattern of seasonal variation in this area is for the fraction of mud to increase during summer and decrease during winter (Baek, 2010). Our field survey data also confirmed this trend (see Table 1 and Fig. 8). In Fig. 8, the mud content is clearly increased in May compared with November. In Fig. 7, the mud-dominant areas in Fig. 7(b) were significantly extended when compared with those in November (Figs. 7(a) and (c)). We also note that the offshore extension of sand in November 2014 was larger than that in the same period of the previous year (November 2013) in Fig. 8, particularly between sites 12 and 24. This feature is also observed in the results in Figs. 7(a) and (c).

Fig. 9(a), Fig. 10(a), and Fig. 11(a) are magnified images of Figs. 7(a), (b), and (c), respectively, in which white dots denote the sampling sites. In winter (November 2013 and 2014), the pattern and trend between the modified PC2 values and measured grain size from ground truth are generally well correlated (Fig. 9(b) and Fig. 11(b)). The correlation coefficients R2 for the two cases are 0.637 and 0.642, respectively (Fig. 9(c) and Fig. 11(c)). However, the relationship in summer (May 2014) between the in situ samples and the image-based estimation was not as good as that in winter. The correlation

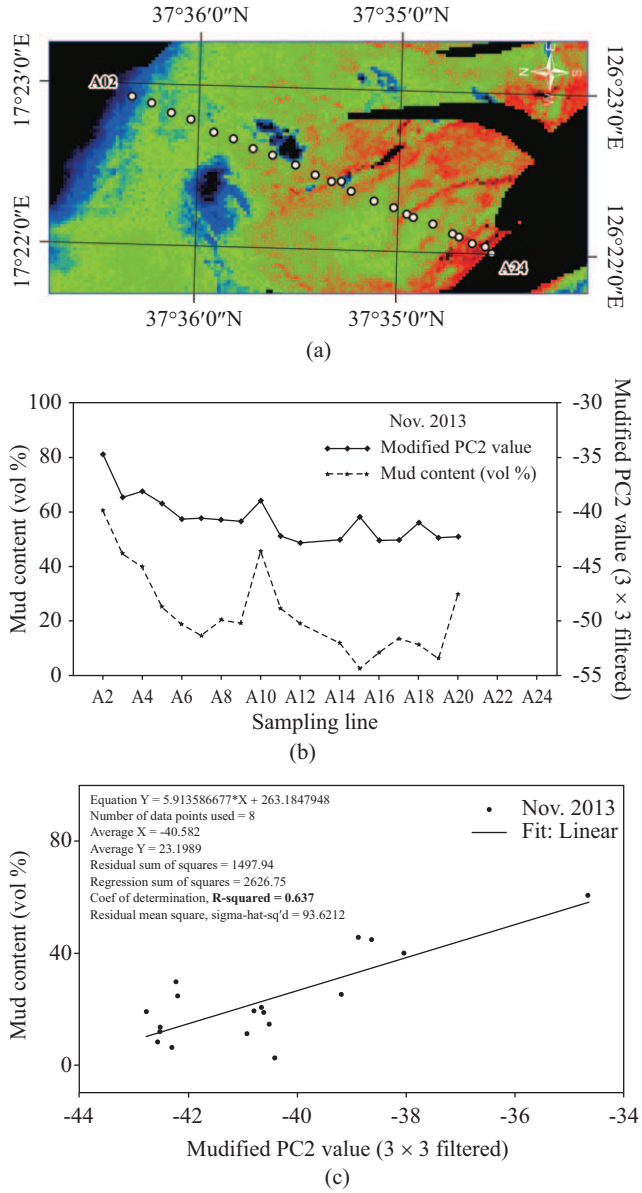

Fig. 9. (a) An enlarged grain size distribution image of Fig. 7(a) around the field survey line in November 2013. (b) Result of the modified PC2 (M-PC2) and mud fraction measured from ground truth data at sampling sites. (c) Correlation between the estimated M-PC2 and the ground truth mud fraction, with a correlation coefficient R2 of 0.64.

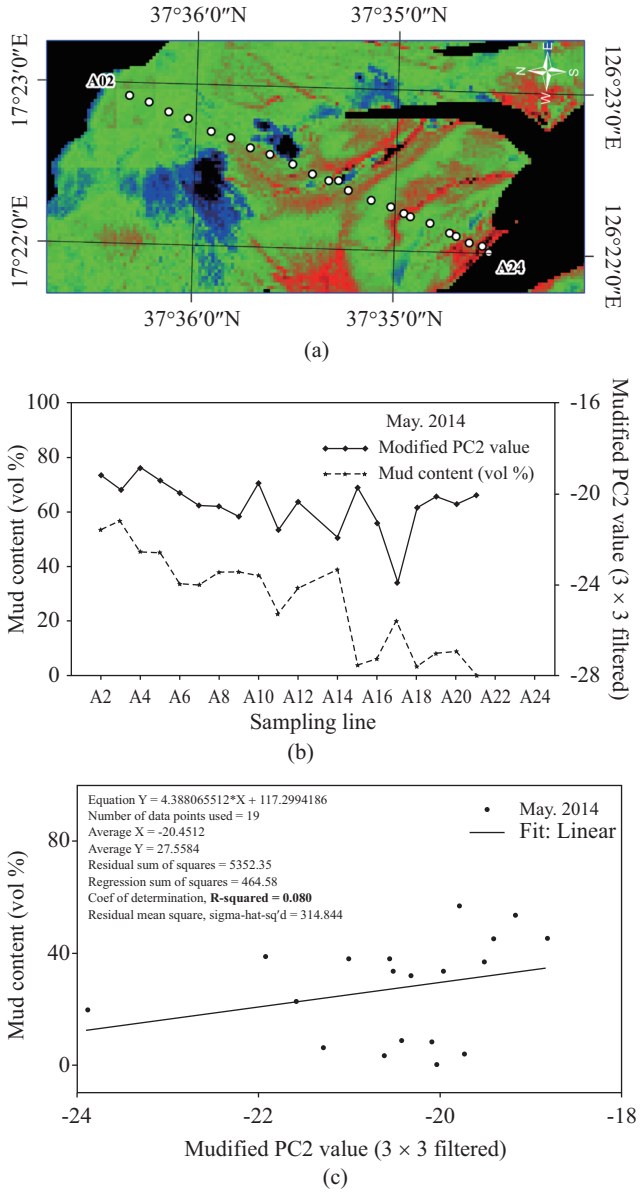

Fig. 10. (a) An enlarged grain size distribution image of Fig. 7(b) around the field survey line in May 2014. (b) Result of the modified PC2 (M-PC2) and mud fraction measured from ground truth data at sampling sites. (c) Correlation between the estimated M-PC2 and the ground truth mud fraction. The correlation coefficient R2 is 0.08, which is much lower than that in winter, possibly because of an inaccurate atmospheric correction under humid conditions.

coefficient R2 is only 0.08 (Fig. 10(c)). This poor correlation can be explained by unfavorable atmospheric conditions in summer. Because the modified PC2 is highly sensitive, inaccurate atmospheric correction contributes substantially to estimation error. However, the variation patterns of mud content along the survey line in Fig. 10(c) are well matched to each other.

Although the application results generally well demonstrate the efficiency and performance of the proposed method, the method faces some limitations that should be accounted for. Although a bare bottom surface is assumed, the intertidal flat surface exhibits features other than grain size and water content, and some of these features cannot be disregarded. First, a significant amount of salt-marsh vegetation develops on some parts of mudflats, for instance in the eastern side of the Ganghwa tidal flats. Thus, this region violates the bare surface assumption of the model, and the biomass would substantially contribute to spectral reflectance. Furthermore, oyster farms are located near site A13, where huge amounts of oyster shell distort the spectral reflectance. This distortion resulted in misclassification

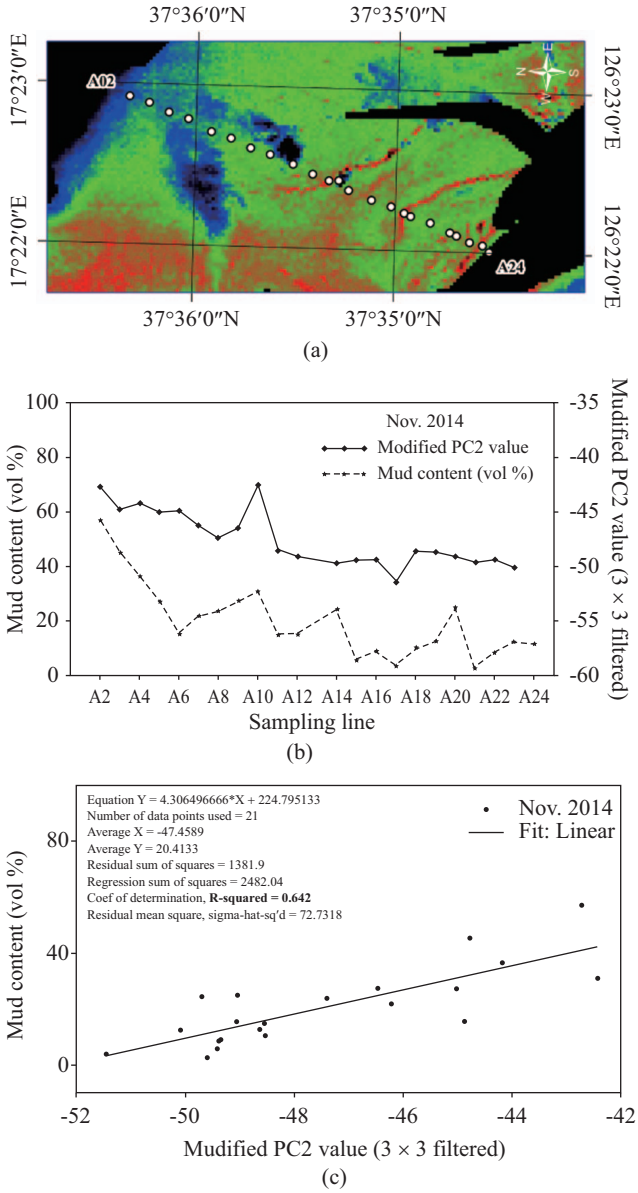

Fig. 11. (a) An enlarged grain size distribution image of Fig. 7(c) around the field survey line in November 2014. (b) Result of the modified PC2 (M-PC2) and mud fraction measured from ground truth data at sampling sites. (c) Correlation between the estimated M-PC2 and the ground truth mud fraction. The correlation coefficient R2 is 0.642, which is similar to that obtained from the anniversary data in November 2013 (Fig. 9).

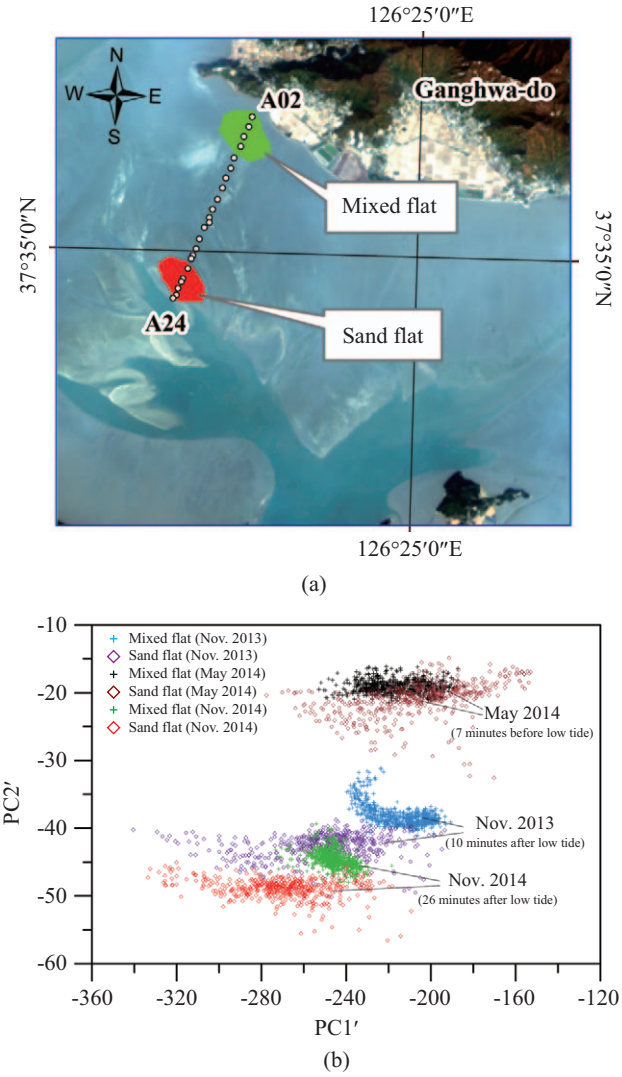

Fig. 12. (a) The locations of typical mixed (green) and sand (red) flats. (b) Scatterplot of the modified PC2 versus PC1, which shows the results from three images acquired at different dates and under different environmental conditions. The two surface types are well distinguished in all three results; however, the absolute values of the modified PC2 differ according to acquisition date.

of grain size as mud because of carbonate-enriched sediment. We will further examine these particular areas in the near future. Second, the surface topography is not quite flat, particularly around tidal channels and creeks, which leads to an irregular BRDF depending on the slope and attitude of the channel banks. This effect must be accounted for in a future study. Third, a normalization method should be developed between different dated images. Fig. 12 shows application results for different dates, which means the atmospheric, solar illumination, and tidal conditions at the time of each OLI image acquisition differed.

As evident in Fig. 12(b), the modified PC2 is very effective for distinguishing between sand and mixed flats under different conditions. However, the absolute values of the modified PC2 differ according to the acquisition date. The atmospheric correction is frequently not adequate for direct and quantitative comparison between different atmospheric conditions. In addition, the reflectance at each pixel is substantially affected by both solar and tidal conditions. The proposed method is limited to distinguishing different surface types within a certain dated image. Therefore, normalization of the resulting modified PC2 by that of a reference date is necessary, and a comparison of an absolute PC2′ value between different dates is only relative to the reference date. Thus, the development of an effective normalization method between different dated images is necessary.

Fourth, considerable percentages of remnant surface water often exist within each ground resolution cell, which extends the algorithm to accommodate a spectral reflectance pattern after critical moisture content, as discussed by Neema et al. (1987) and Liu et al. (2001). Ryu et al. (2002) proposed a schematic model associated with the spectral reflectance of the tidal flat in which the remnant water scattered on the surface after exposure is emphasized as an additional factor. However, accounting for this effect on a pixel-by-pixel basis remains problematic. We should consider the effects of not only bulk water content but also residual surface water on the optical reflectance.

IV. CONCLUSIONS

A two-step PCA (or modified PCA) method was proposed for classification of sediment within intertidal flats from remotely sensed optical reflectance data. The core idea was to build new water-content-independent PCA components via three-dimensional axis rotation of the original PCA axes. A great advantage of the method lies in the fact that the model enables classification of intertidal flat sediment into mud (< 63 μm in grain size) and sand (> 63 μm in grain size) solely on the basis of optical reflectance, regardless of water content. The developed model was applied to LANDSAT-8 OLI images over the Ganghwa tidal flats, South Korea; the results demonstrate the effectiveness of the method in terms of grain size distribution and seasonal change in sediment.

Although the proposed method is very useful for sediment classification within intertidal flats, some limitations exist. First, the method does not account surfaces other than bare sediment, such as salt-marshes or other biomass. Second, it does not consider topographic effects, which are particularly prevalent near intertidal channels and creeks where the slope and attitude abruptly change. Third, it requires a normalization method for quantitative comparison between different data. Fourth, the effect of remnant surface water is not adequately accounted for because remnant surface water is frequently observed within intertidal flats. The model also requires reliable atmospheric correction because the modified PC2 component is very sensitive to the atmospheric conditions. Although the proposed method still requires further refinement, the application results clearly demonstrate the potential of the approach for intertidal flat surface sediment classification solely from remotely measured optical reflectance data. In the near future, we will further extend the method to accommodate ocean color sensors on geostationary satellites such as Geostationary Ocean Color Imager (GOCI).

ACKNOWLEDGEMENTS

This research was part of the project titled “Development of Geostationary Ocean Color Imager (GOCI) Land Products for Long-term Monitoring of Tidal Flats and Arid Lands” funded by the Korea Institute of Ocean Science and Technology (KIOST).

REFERENCES

Baek, Y. S., J. K. Kim and S. S. Chun (2010). Seasonal sedimentation of intertidal flat revealed by distribution of ichnofacies: Southern tidal flat (Yeochari) of Ganghwa Island. Journal of the Geological Society of Korea, 46(6), 661-674. (in Korean)

Chen, L. C. and J. Y. Rau (1997). Detection of shoreline changes for tideland areas using multi-temporal satellite images. International Journal of Remote Sensing 19(17), 3383-3397.

Cooper, C. D. and J. F. Mustard (1999). Effects of very fine particle size on reflectance spectra of smectite and palagonitic soil. Icarus, 142, 557-570

Cracknell, A. P. (1999). Remote sensing techniques in estuaries and coastal zones: An update. International Journal of Remote Sensing 19(3), 485-496.

Choi, K. S. and R. W. Dalrymple (2004). Recurring tide-dominated sedimentation in Kyonggi Bay (west coast of Korea): similarity of tidal deposits in late Pleistocene and Holocene sequences. Marine Geology 212, 81-96.

Doerffer, R. and D. Murphy (1989). Factor analysis and classification of remotely sensed data for monitoring tidal flats. Helgoländer Meeresunters 43, 275-293

Folk, R. L. (1966). A review of grain size parameters. Sedimentology 6, 73-93.

Liu, W, F. Bareta, X. Gu, Q. Tong, L. Zheng and B. Zhang. (2001). Relating soil surface moisture to reflectance. Remote Sensing of Environment 81, 238-246.

Neema, D. L., A. Shah and N. Patel (1987). A statistical optical model for light reflection and penetration through sand. International Journal of Remote Sensing 8(8), 1209-1217.

Rainey, M. P., A. N. Tyler, R. G. Bryant, D. J. Gilvear and P. McDonald (2000). The influence of surface and interstitial moisture on the spectral characteristics of intertidal sediments: implications for airborne image acquisition and processing. International Journal of Remote Sensing 21(16), 3025-3038.

Rainey, M. P., A. N. Tyler, D. J. Gilvear, R. G. Bryant and P. McDonald (2003). Mapping intertidal estuarine sediment grain size distributions through airborne remote sensing. Remote Sensing of Environment 86, 480-490.

Ryu, J. H., Y. H. Na, J. S. Won and R. Doerffer (2004). A critical grain size for Landsat ETM+ investigations into intertidal sediments: a case study of the Gomso tidal flats, Korea. Estuarine, Coastal and Shelf Science 60, 491-502.

Ryu, J. H., J. S. Won and K. D. Min (2002). Waterline extraction from Landsat TM in a tidal flat: A case study in Gomso Bay, Korea. Remote Sensing of Environment 83, 443-457.

Tyler, A. N., D. C. W. Sanderson, E. M. Scott and J. D. Allyson (1996). Accounting for spatial variability and fields of view in environmental gamma ray spectrometry. Journal of Environmental Radioactivity 33, 213-235.

Wentworth, C. K. (1922). A Scale of Grade and Class Terms for Clastic Sediments. The Journal of Geology 30(5), 377-392.

Woo, H. J and J. G. Je (2002). Changes of sedimentary environments in the southern tidal flat of Kanghwa island. Ocean Polar Research 24, 331-343. (in Korean)